



STRUCTURAL SCIENCE
CRYSTAL ENGINEERING
MATERIALS

Volume 73 (2017)

Supporting information for article:

**Multi-temperature study of potassium uridine-5'-monophosphate:
electron density distribution and anharmonic motion modelling**

**Katarzyna N. Jarzemska, Katarzyna Ślepokura, Radosław Kamiński, Matthias J.
Gutmann, Paulina M. Dominiak and Krzysztof Woźniak**

1S. Full experimental section

1.1S. Materials. UMPH₂ was purchased from Sigma-Aldrich Co. K(UMPH) was obtained by reacting UMPH₂ with KHCO₃ in 1-to-1 molar ratio. Both substrates were initially dissolved in water. In the next stage the majority of water was evaporated under dry nitrogen, and the final product was crystallised from the remaining solution with an additive of methanol. Such a procedure resulted in crystals of excellent quality which were subjected to further X-ray diffraction studies. We note that no single crystals were obtained from pure water.

1.2S. Data collection and processing. A charge-density-quality single crystal of suitable size was chosen for the purpose of the current study, thus, multi-temperature data collections at 10 K, 100 K, 200 K and 300 K were performed on one single crystal. The 100 K, 200 K and 300 K data sets were collected using a Bruker AXS Kappa APEX II Ultra single-crystal diffractometer equipped with a CCD-type APEX II area detector, molybdenum TXS rotating anode (Mo-K α radiation, $\lambda = 0.71073 \text{ \AA}$), 4-circle goniometer, multi-layer optics, and an Oxford Cryosystems low-temperature nitrogen gas-flow device (700 Series Cryostream). The 10 K data set was collected at an equivalent setup (the only

difference being a 3-circle goniometer), while the low temperature was obtained with the Cryo Industries of America He-flow device (Cryocool-LHe). Particular care was taken to record all low-angle reflections, which are crucial for reliable charge density determination, and to minimise the number of reflections with $I/\sigma(I) < 3.0$ in the whole data set. It is worth mentioning that the collected reflection data were of high quality with well-defined round reflections, and the crystal exhibited very low mosaicity. The latter was indicated by the fact that two nearly *identical* data sets measured at 100 K differing only in the single-frame scan width (0.50° vs. 0.25°) gave results in favour of the thinner reflection slicing (R_{mrg} was twice smaller for 0.25° scan data set). This is in line with the previous literature studies on data quality with respect to the scan width (Sørensen & Larsen, 2003).

The determination of the unit cell parameters and the integration of raw diffraction images were performed with the *APEX3* program package (Bruker AXS, 2015). The data set was corrected for Lorentz, polarization and oblique incidence effects. The multi-scan absorption correction, frame-to-frame scaling and merging of reflections were carried out with the *SORTAV* program (Blessing, 1987, 1995, 1997). All data sets exhibited high resolution limit of $(\sin \theta / \lambda)_{\text{max}} \approx 1.2 \text{ \AA}^{-1}$, and overall completeness of more than 90%. Final data collection and reduction parameters are summarised in Table 1. Furthermore, selected sets of raw diffraction frames and associated data are available online under the following DOI: 10.18150/repod.7426818 (Repository for Open Data, Interdisciplinary Centre for Mathematical and Computational Modelling, University of Warsaw, Warsaw, Poland).

1.3S. Structure solution and refinement. In all cases the crystal structure was solved by a charge-flipping method (Oszlányi & Sütő, 2004, 2005; Palatinus, 2013) with the *SUPERFLIP* program (Palatinus & Chapuis, 2007). Initial independent atom model (IAM) refinements were performed with the *JANA* program (Petříček *et al.*, 2014).

Multipole refinements for all data sets were carried out using the *MOPRO* suite (Guillot *et al.*, 2001; Jelsch *et al.*, 2005) combined with the current version of the University at Buffalo Data Bank (UBDB) (Jarzemska & Dominiak, 2012), which employs the Hansen-Coppens multipole model (Hansen & Coppens, 1978). In this formalism, the total atomic electron density (of the k -th atom) is the sum of three components:

$$\rho_k(\mathbf{r}) = \rho_{ck}(r) + P_{vk}\kappa_k^3\rho_{vk}(\kappa r) + \sum_{l=0}^{l_{\max}} \sum_{m=-l}^l P_{klm}\kappa'_{kl}{}^3 R_{kl}(\kappa'_{kl}r) d_{klm}(\theta, \varphi)$$

where ρ_{ck} and ρ_{vk} are spherical core and valence densities, respectively. The third term contains the sum of angular functions (d_{klm}) which model aspherical deformations. The angular functions d_{klm} consist of real spherical harmonic functions normalised to the electron density. The coefficients P_{vk} and P_{klm} stand for multipole populations of the valence and deformation density multipoles, respectively. Radial function (R_{kl}) is defined as:

$$R_{kl}(r) = \frac{\zeta_{kl}^{n_{kl}+3}}{(n_{kl} + 3)!} r^{n_{kl}} \exp(-\zeta_{kl}r)$$

where ζ_{kl} and n_{kl} are parameters assigned to each element type separately. κ_k and κ'_{kl} are scaling parameters, which control the expansion and contraction of the valence spherical and deformation densities, respectively. In this contribution each atom was assigned with the core and spherical-valence scattering factors derived from Su & Coppens, and Macchi & Coppens wave functions (Su & Coppens, 1998; Macchi & Coppens, 2001). In the Hansen-Coppens formalism, P_{vk} , P_{klm} , κ_k , and κ'_{kl} (these usually are constrained to be equal for all l values) are the refineable parameters together with the atomic coordinates and thermal motion coefficients. All the performed refinements were based on F , while only reflections fulfilling the $I \geq 3\sigma(I)$ criterion were taken into account. Such a cut-off does not influence the final model significantly, as has been shown recently (results obtained with and without cut-off are within the method's precision) (Kamiński *et al.*, 2014). Furthermore, for all data sets the number of reflections not fulfilling this criterion was equal 3%, 5%, 18% and 33% for the 10 K, 100 K, 200 K and 300 K data sets, respectively. In view of the above, an additional test refinement without the cut-off was conducted for the 300 K data set, since the lack of about 33% of data may significantly bias the final results (*e.g.* biased thermal parameters enforce errors on the static electron density through the incomplete deconvolution of the two). Nevertheless, it appeared that the obtained models were quite alike, thus further analyses were carried out on the primary model derived with the applied cut-off (see Table 2S and Figure 2S for comparison). The statistical weights were used (*i.e.* for i -th reflection $w_i = 1/\sigma_i^2$). Initial atomic coordinates, x , y , and z , and anisotropic displacement parameters (U_{ij} 's) for each atom were taken from the independent-atom-model-based refinement, whereas the initial multipolar and contraction-expansion parameters were transferred from UBDB

with the aid of the *LSDB* program (Volkov *et al.*, 2004; Jarzemska & Dominiak, 2012). Additionally, *LSDB* standardises the X–H bond lengths (X = non-hydrogen atom) to neutron-normalised distances according to the values tabulated by Allen & Bruno (*e.g.* $d_{\text{O–H}} = 0.970 \text{ \AA}$ (ribose fragment), $d_{\text{O–H}} = 1.015 \text{ \AA}$ (phosphate fragment), $d_{\text{N–H}} = 1.030 \text{ \AA}$) (Allen *et al.*, 1987; Allen & Bruno, 2010). The *MOPRO* program allows for applying specific restraints during the refinement. Therefore, in the *initial* stage, the hydrogen atom U_{iso} parameters (*i.e.* isotropic thermal parameters) were restrained to the values of $1.2 \cdot U_{\text{eq}}^{\text{X}}$ or $1.5 \cdot U_{\text{eq}}^{\text{X}}$ (for X = C or O/N, respectively) with $\sigma = 0.01$ (an appropriate restraint weight is equal to $1/\sigma^2$). In the *subsequent* stages of the refinement, the estimation of anisotropic hydrogen atom ADPs (atomic displacement parameters) for all data sets was realised using the *SHADE* server (Madsen, 2006; Munshi *et al.*, 2008). It should be stressed that *SHADE*-estimated values were used also in the case of the 10 K data, as not all hydrogen atom ADPs were of satisfactory quality (the time-of-flight neutron diffraction experiment was quite demanding due to the low scattering power of the sample and the structure’s complexity). In turn, the X–H bond lengths for 10 K data set were restrained to neutron-derived distances with $\sigma = 0.001$. Similarly, for all other data sets, X–H bond lengths were restrained to neutron-normalised values with the same σ value. Even in the absence of the neutron data for higher temperatures, such an approach has been successfully applied in a variety of experimental charge density studies (Jelsch *et al.*, 2000; Chęcińska *et al.*, 2006; Meindl *et al.*, 2009; Jørgensen *et al.*, 2013; Jarzemska *et al.*, 2013; Jarzemska *et al.*, 2014). However, we note that the neutron-derived X–H bond lengths determined at 10 K were very close to the averaged values reported by Allen & Bruno (Allen, 2002; Allen & Bruno, 2010). The multipole expansion was truncated at the hexadecapole ($l_{\text{max}} = 4$) and quadrupole ($l_{\text{max}} = 2$) levels for all non-hydrogen and hydrogen atoms, respectively. In the case of hydrogen atoms such model when coupled with the *SHADE* approach was proven to give best results (Hoser *et al.*, 2009). All κ' parameters were kept fixed at the UBDB-transferred values (we note that κ and κ' for potassium were kept fixed at the value of 1.0). All atomic deformation density functions were subjected to the local symmetry constraints, imposed by the *LSDB* program. In the case of hydrogen atoms, solely the bond-directed dipole and quadrupole populations (*i.e.*, P_{10} and P_{20}) were refined. The importance of proper treatment of local symmetry constraints and restraints in charge density studies has been already emphasized in a set of research papers (Zarychta *et al.*, 2011; Paul *et al.*, 2011; Poulain-Paul *et al.*, 2012).

In the previous works by Starynowicz and co-workers (Janicki & Starynowicz, 2010; Mermer & Starynowicz, 2011, 2012; Starynowicz & Lis, 2014; Mermer *et al.*, 2015), the authors used the n_l and ζ_l parameters for the phosphorus atom equal to 6 and 2.7456 a_0^{-1} , respectively (the same for all $l = 1,2,3,4$). Such proceedings were based on the previous report by Espinosa *et al.* (Espinosa *et al.*, 1996). However, in our case (when confronting different models refined against the 100 K data set) applying these parameters resulted in a *slightly* worse fit as compared to that employing the standard ones as suggested by the *XD* program internal routine (Volkov *et al.*, 2016) ($n_l = 4$, $\zeta_l = 3.4590 \text{ a}_0^{-1}$). However, we note that there is still no common agreement (Moss *et al.*, 1995; Souhassou *et al.*, 1995; Yufit *et al.*, 2000; Kinzhybalo *et al.*, 2013) on which parameters one should use for the phosphorus atom to get the best possible results within the multipolar approximation. Furthermore, for the sake of further analysis it was particularly important to verify the approach to the refinement of the potassium ion. The refinement with standard atomic scattering factors (K^0 : [core: $1s^2 2s^2 3s^2 2p^6 3p^6$, valence: $4s^1$] or [core: $1s^2 2s^2 3s^2 2p^6$, valence: $3p^6 4s^1$]) led to non-physical results (*e.g.* integrated AIM charges outside chemically-sensible limits). In some of the published works (Koritsanszky *et al.*, 2000; Nelyubina *et al.*, 2009; Mermer & Starynowicz, 2012) the P_v parameter was constrained to a specified value. In our case, an acceptable model was obtained with the ionic scattering factor having $3p$ electrons moved to the valence shell (K^+ : [core: $1s^2 2s^2 3s^2 2p^6$, valence: $3p^6$]). In addition, the n_l and ζ_l parameters for this atom were equal to 4 and 5.1504 a_0^{-1} , respectively, as by default suggested by the *XD* package. On the other hand, there still remains the question if the potassium atom is spherical or not. When compared with much more rigid lithium or sodium atoms, it possesses more electrons and is generally known as being more polarisable (Molof *et al.*, 1974; Ekstrom *et al.*, 1995; Holmgren *et al.*, 2010). To the best of our knowledge, in the available literature potassium was most often considered as being spherical (Koritsanszky *et al.*, 2000; Nelyubina *et al.*, 2009; Mermer & Starynowicz, 2012). Nevertheless, in the advent of crystallography and experimental methods, which allow for collecting high quality data, it is tempting to extract and model on heavy atoms any aspherical deformations present. This is especially interesting considering the latest reports on core deformation effects suggested on the basis of experimental charge density data (Fischer *et al.*, 2011; Zhurov & Pinkerton, 2013; Bindzus *et al.*, 2014). Therefore, both possibilities were investigated, *i.e.* treating potassium as spherical (with

only the P_v parameter refined), or aspherical (with multipole expansion applied to the hexadecapole level). Obviously, the aspherical model gives a slightly better fit, reflected in lower R -factors and residual density values (for numerical details see Supplementary Materials). This is due to the larger number of refined parameters. On the other hand, differences are really small, and both models yield very similar integrated AIM charges for potassium (+0.70 e (10 K) / +0.59 e (100 K), and +0.68 e (10 K) / +0.59 e (100 K), for spherical and aspherical models, respectively). In order to decide which model is more physically sound we compared electron distribution on the potassium centre in both models (for 10 K data set), spherical (Figure 1a) and aspherical (Figure 1b), with that obtained by theoretical periodic computations (Figure 1c). The latter, theoretical results, further described in details, are treated here as an independent reference. The theory-computed negative Laplacian map clearly shows the absence of noticeable valence-shell charge concentrations (VSCCs) in the potassium outer shell. Such a theoretical outcome best supports the spherical multipole model for the potassium ion. In the case of the 100 K data set the effect is similar, but less pronounced. Consequently, in all models derived for the purpose of this study the spherical description of the potassium ion was applied. We note here that to make the 300 K charge density model reasonable, the P_v parameter for the potassium centre was restrained to the value of 6.3 e with $\sigma = 0.01$ (based on the results from the lower-temperature data sets).

Despite the very low residual density extreme values obtained for models at all temperatures and satisfactory R -factors (considering non-trivial description of potassium and phosphorus atoms), careful inspection of the residual density for 100 K, 200 K and 300 K data sets revealed some systematic effects within the uracil fragment. While the details are described in the following section of this paper, we note here that we were able to take these effects into account by refining the 3rd-order Gram-Charlier parameters (Johnson, 1969; Kuhs, 1983; Scheringer, 1985), C_{jkl} , introduced in the form:

$$T(\mathbf{h}) = T_0(\mathbf{h}) \left[1 - i \frac{4\pi^3}{3} \sum_j \sum_k \sum_l C_{jkl} h_j h_k h_l \right]$$

where $T_0(\mathbf{h})$ is the harmonic temperature factor, and h_k represents the k -th component of the scattering vector \mathbf{h} . The physical reliability of the anharmonic model was confirmed by the probability density function (PDF) computed with the *JANA* program. Furthermore, the absence of these effects in the 10 K data set (anharmonic effects for

non-hydrogen atoms are expected to diminish significantly with temperature lowering) additionally supports such data treatment. The refined anharmonic parameters appeared to be rather weakly correlated with multipolar parameters (the average correlation coefficient was equal to about 0.45 for all data sets). The maximum was equal to 0.75, 0.81 and 0.81 for 100 K, 200 K and 300 K data sets, respectively. It was always the C_{222} vs. Y -oriented dipole, for the O9 oxygen atom. Also, correlation with positional and thermal parameters is rather low (about 0.6 on average), while the number of larger (anti)correlations increases with temperature. All these results are in line with many recent literature reports on this matter (Scheins *et al.*, 2010; Zhurov *et al.*, 2011; Herbst-Irmer *et al.*, 2013; Poulain *et al.*, 2014), where high-quality data allow for reliable deconvolution of electron density and thermal motion features.

Considering all the above, the general strategy consisted of the following refinement steps: the refinement of (i) scale factor (which was also refined in almost all other stages); (ii) atomic coordinates; (iii) atomic coordinates and ADPs; (iv) *SHADE* estimation of anisotropic hydrogen atom ADPs (which was also updated in-between other stages until convergence); (v) multipole population parameters in a stepwise manner; (vi) all multipole population parameters and structural parameters simultaneously; (vii) block refinement of non-hydrogen atom κ parameters (1st block), step no. (vi) (2nd block); (viii) all parameters from step no (vii) together; (ix) block refinement of non-hydrogen atom κ parameters (1st block), step no. (vi) (2nd block), and 3rd order anharmonic parameters for the C7, C8, C9 and O9 atoms (no scale factor was refined at this stage; $(\sin \theta / \lambda) \geq 0.8 \text{ \AA}^{-1}$) (3rd block); (x) all parameters simultaneously.

In general, determination of absolute structure was not needed due to the known configuration of the studied compound (β -D-ribofuranose ring). However, as a test, the Flack parameter was determined in each case. Its value appeared to be very close to zero, equal +0.005(6), -0.002(4), -0.002(5) and +0.001(6) for the 10 K, 100 K, 200 K and 300 K data sets, respectively, which supported the mentioned choice of the absolute configuration. The Flack parameter was derived here based on the method proposed by Hooft *et al.* (Hooft *et al.*, 2008), and implemented in the *PLATON* software (Spek, 2002). The above analysis applies to the final multipole models with reflections fulfilling the $I \geq 3\sigma(I)$ condition. It should be noted, that in the case of a relatively strong anomalous signal (K and P atoms present) and wrong choice of absolute configuration, multipole refinement would not be possible.

The differences of mean-square displacement amplitudes computed along bonds for all covalently-bound non-hydrogen-atom pairs fulfilled the so-called ‘rigid-bond’ test, except for the C7–O9 bond in the 300 K data set, for which the obtained value was equal to exactly 10^{-3} \AA^2 which is at the edge of the commonly accepted criterion (Hirshfeld, 1976). Residual density properties were evaluated with the *JNK2RDA* program (Meindl & Henn, 2008). The analysis shows that the derived models are characterised by rather flat and almost featureless residual density distribution (small ‘shoulders’ visible in Figure 3S for the 10 K data set result most probably from the higher residual density regions near the K and P atoms). It should be noted that for the 300 K data set the high-angle weak reflections (*i.e.* with $I < 3\sigma(I)$) are characterized by the increased observed-to-calculated structure factor ratios for $\sin \theta / \lambda > 1.1 \text{ \AA}^{-1}$ (Figure 4S). In this view, the possible thermal diffuse scattering (TDS) contribution, which may be significant at high angles and at elevated temperatures, should be examined. Since we could not modify the integration program, we studied the effect by applying the procedure proposed by Niepötter *et al.* (Niepötter *et al.*, 2015). Thus, instead of modifying the original set of structure factors we introduced the polynomial scale factor available in the *MOPRO* program. Nonetheless, multiple trials did not lead to a model with the diminished ‘tail’ observed in the scale plot. Therefore, next the influence of these weak reflections onto the refined model was checked. The refinement with the $\sin \theta / \lambda \leq 1.1 \text{ \AA}^{-1}$ cut-off was carried out but no significant differences were found. All this leads to a conclusion that the TDS effect is either rather small, or cannot be corrected with such a simple procedure in this particular case. The observed discrepancy between model and the data observed for the high-angle weak reflections can be also attributed to other factors, such as problems with the data scaling, or the mentioned incomplete deconvolution.

The final note concerns the empirical rule proposed by Kuhs (Kuhs, 1992, 1988). In the case of all atoms, where we included the 3rd-order Gram-Charlier parameters, the rule of the minimal $\sin \theta / \lambda$ requirement allowing for a ‘reliable’ refinement of anharmonic motion parameters was fulfilled. We stress, however, the rule can be too strict when the Gram-Charlier parameters are refined for heavier atoms (Herbst-Irmer *et al.*, 2013). Here, it was obviously not the case.

All the final refinement statistics are summarized in Table 1. The CIF files are present in the Supplementary Materials, or can be retrieved from the Cambridge Structural Database (CSD) (Groom *et al.*, 2016) (deposition numbers: CCDC 1533598-1533601).

1.4S. Neutron diffraction. A single-crystal time-of-flight neutron diffraction experiment was performed at the SXD beamline (Keen *et al.*, 2006), at the neutron spallation source at the ISIS facility (Oxfordshire, UK). For the purpose of the experiment a single crystal of size approximately equal to $1 \times 1 \times 2 \text{ mm}^3$ was attached to an Al pin with an adhesive Al tape, and cooled to 10 K in a closed-cycle refrigerator with He as an exchange gas. 11 crystal orientations were recorded in total, each exposed for 8 – 16 hours. We note that the last 3 orientations were collected simultaneously for 3 crystals of the same size (Wilson, 1997). Data reduction was accomplished using the locally available *SXD2001* program (Keen *et al.*, 2006). The crystal structure (with anisotropic hydrogen-atom thermal parameters) was then refined in the *JANA* package directly from the time-of-flight data. It is also worth noting that the extinction was successfully modelled by the Becker-Coppens approach (Becker & Coppens, 1974b, a, 1975). Selected parameters: $a = 8.0754(16) \text{ \AA}$, $b = 10.387(2) \text{ \AA}$, $c = 16.000(3) \text{ \AA}$; total no. of reflections: 13658; no. of reflections with $I \geq 3\sigma(I)$: 13558; index ranges: $-19 \leq h \leq 21$, $-28 \leq k \leq 23$, $-23 \leq l \leq 44$; no. of parameters: 318; discrepancy factors: $R[F] (I \geq 3\sigma(I)) = 8.11\%$, $wR[F] (I \geq 3\sigma(I)) = 8.68\%$, $R[F] (\text{all data}) = 8.27\%$, $wR[F] (\text{all data}) = 8.85\%$, goodness of fit (S) ($I \geq 3\sigma(I)$) = 2.74; nuclear density largest extrema: $-4.13/+4.90 \text{ fm} \cdot \text{\AA}^{-3}$; extinction parameter (type I Lorentzian isotropic): 10.0(3). The CIF file is available in the Supplementary Materials, or can be retrieved from the CSD (deposition number: CCDC 1533597). Raw neutron diffraction frames and associated data are available online under the following DOI: 10.18150/repod.6850518 (Repository for Open Data).

Table 1S. Selected parameters describing the most important models tested.**M1a-H** – model with spherical potassium, harmonic (* same but refined on F^2)**M1b-H** – same as M1aH but with different radial function for phosphorus, harmonic**M2-H** – model with aspherical potassium, harmonic**M1a-AN** – model with spherical potassium, anharmonic (** same but refined on all data)**M2-AN** – model with aspherical potassium, anharmonic

<i>10 K data set</i>					
<i>Parameter</i>	M1a-H (*)	M1b-H	M2-H	M1a-AN	M2-AN
P_V (K1)	6.25(3)	–	6.27(3)	–	–
P_V (P1)	4.14(7)	–	4.12(7)	–	–
Q_{AIM} (K1)	+0.70	–	+0.68	–	–
Q_{AIM} (P1)	+2.91	–	+2.94	–	–
$\Delta q_{res}^{min} / \Delta q_{res}^{max}$ ($I \geq 3\sigma(I)$)	-0.16 / +0.15	–	-0.13 / +0.12	–	–
$\Delta q_{res}^{min} / \Delta q_{res}^{max}$ (all data)	-0.16 / +0.15	–	-0.14 / +0.12	–	–
$R[F]$ ($I \geq 3\sigma(I)$) / (all data)	1.48% / 1.54%	–	1.44% / 1.51%	–	–
	(* 1.47% / 1.54%)				
$wR[F]$ ($I \geq 3\sigma(I)$) / (all data)	1.80% / 1.84%	–	1.76% / 1.80%	–	–
	(* 1.80% / 1.84%)				
$R[F^2]$ ($I \geq 3\sigma(I)$) / (all data)	2.41% / 2.41%	–	1.76% / 2.35%	–	–
	(* 2.40% / 2.40%)				
$S[F]$ ($I \geq 3\sigma(I)$) / (all data)	0.836 / 0.840	–	0.820 / 0.824	–	–
<i>100 K data set</i>					
<i>Parameter</i>	M1a-H	M1b-H	M2-H	M1a-AN	M2-AN
P_V (K1)	6.36(3)	6.40(3)	6.36(3)	6.37(3)	6.37(3)
P_V (P1)	4.16(6)	4.26(6)	4.17(6)	4.26(6)	4.27(6)
Q_{AIM} (K1)	–	–	–	+0.59	+0.59
Q_{AIM} (P1)	–	–	–	+2.93	+2.94
$\Delta q_{res}^{min} / \Delta q_{res}^{max}$ ($I \geq 3\sigma(I)$)	-0.10 / +0.11	-0.10 / +0.11	-0.10 / +0.11	-0.07 / +0.06	-0.07 / +0.06
$\Delta q_{res}^{min} / \Delta q_{res}^{max}$ (all data)	-0.11 / +0.11	-0.11 / +0.11	-0.11 / +0.11	-0.08 / +0.08	-0.08 / +0.08
$R[F]$ ($I \geq 3\sigma(I)$) / (all data)	1.20% / 1.32	1.20% / 1.33%	1.19% / 1.31%	1.11% / 1.24%	1.10% / 1.23%
$wR[F]$ ($I \geq 3\sigma(I)$) / (all data)	1.52% / 1.56	1.53% / 1.57%	1.51% / 1.56%	1.41% / 1.45%	1.40% / 1.44%
$R[F^2]$ ($I \geq 3\sigma(I)$) / (all data)	1.74% / 1.75	1.75% / 1.77%	1.72% / 1.73%	1.61% / 1.63%	1.59% / 1.61%
$S[F]$ ($I \geq 3\sigma(I)$) / (all data)	0.911 / 0.913	0.914 / 0.915	0.907 / 0.908	0.844 / 0.848	0.840 / 0.844
<i>300 K data set</i>					
<i>Parameter</i>	M1a-H	M1b-H	M2-H	M1a-AN (**)	M2-AN
$R[F]$ ($I \geq 3\sigma(I)$) / (all data)	–	–	–	1.94% / 3.36%	–
				(**1.94% / 3.35%)	
$wR[F]$ ($I \geq 3\sigma(I)$) / (all data)	–	–	–	2.22% / 2.63%	–
				(**2.22% / 2.63%)	
$R[F^2]$ ($I \geq 3\sigma(I)$) / (all data)	–	–	–	2.70% / 2.87%	–
				(* 2.71% / 2.87%)	

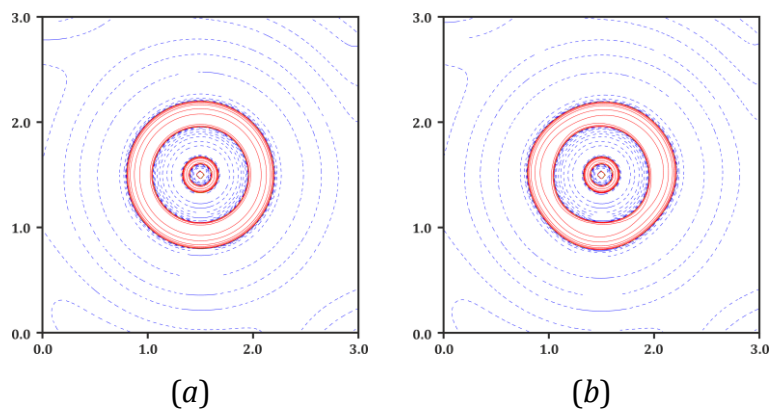


Figure 1S. Electron density Laplacian maps in the vicinity of the potassium ion for multipole models with spherically (*a*) and aspherically (*b*) refined potassium fragment (the 100 K data set; logarithmic contours; blue dashed lines – positive values, red solid lines – negative values; K1-04-02 plane).

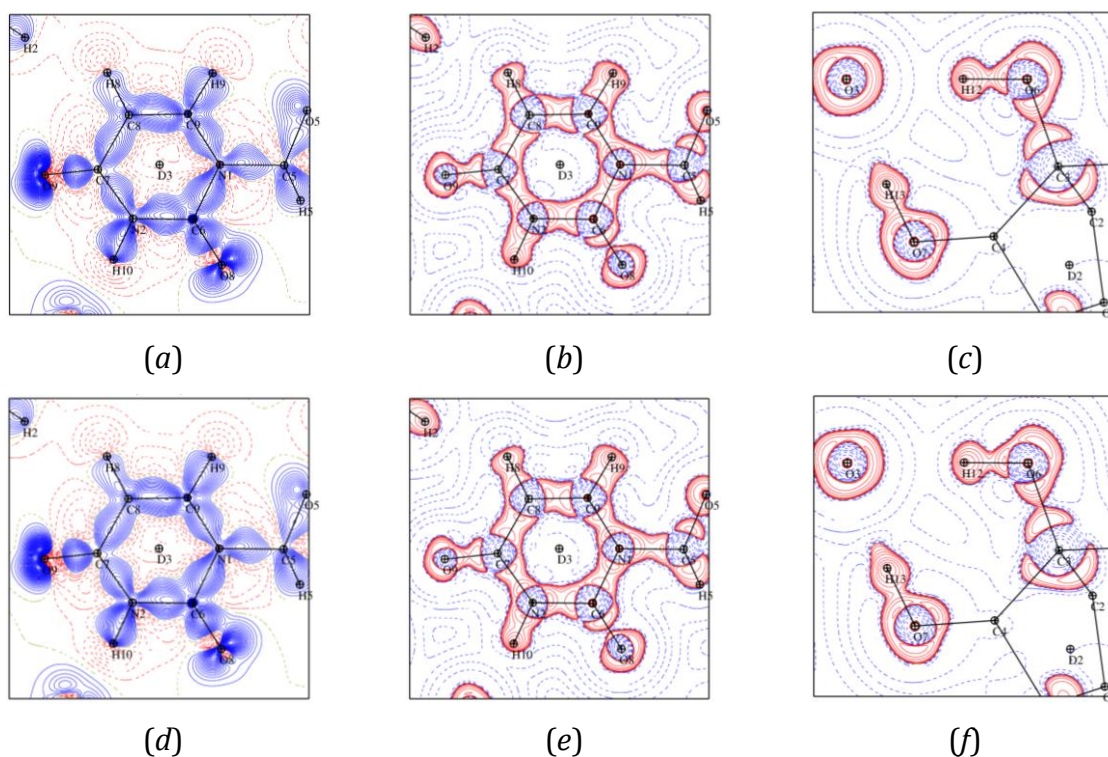


Figure 2S. Deformation and Laplacian maps for selected fragments derived from the 300 K data set: (*a-c*; upper panels) refinement with the cut-off, and (*d-f*; bottom panels) refinement on all data. Figures (*a,b*) are the same as Figures 6 and 7 present in the main body of the manuscript, whereas figures (*c,f*) represent the same fragment as in Figure 5.

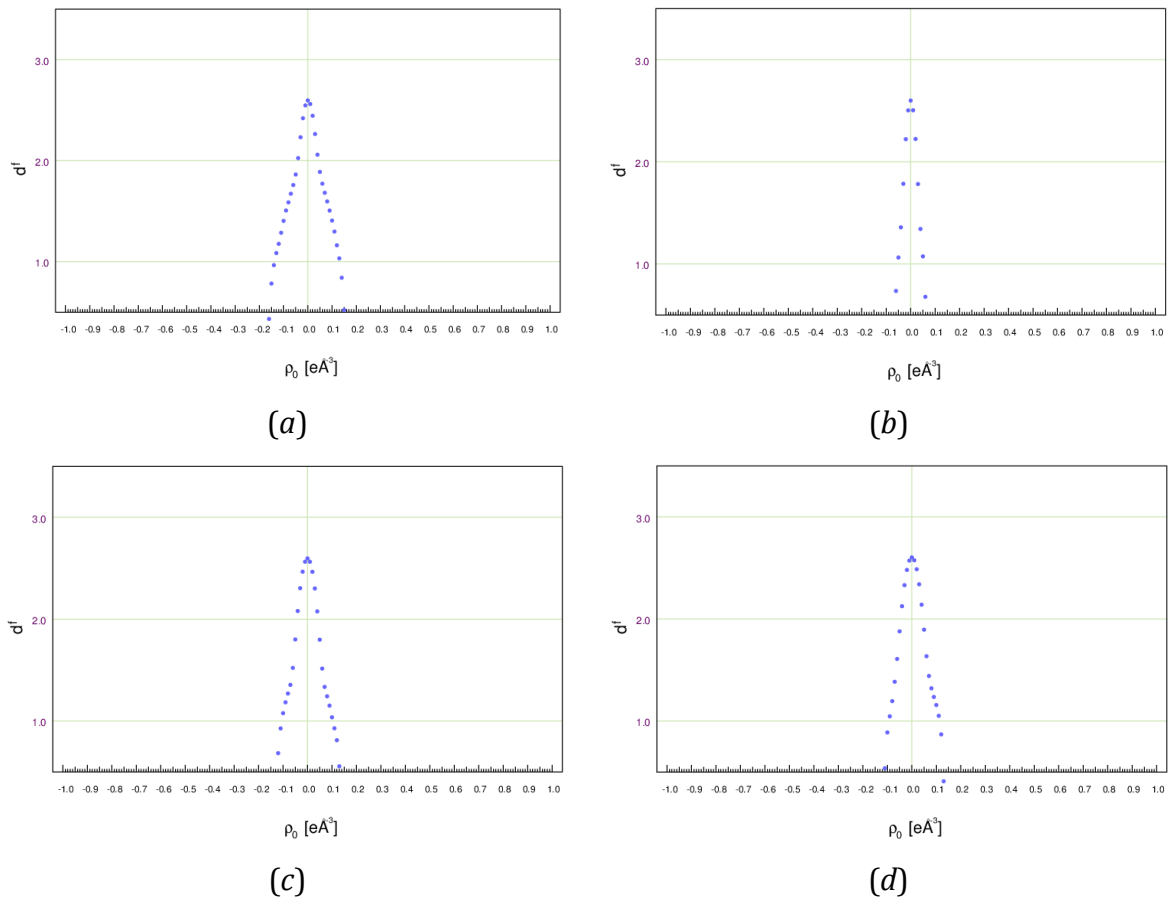
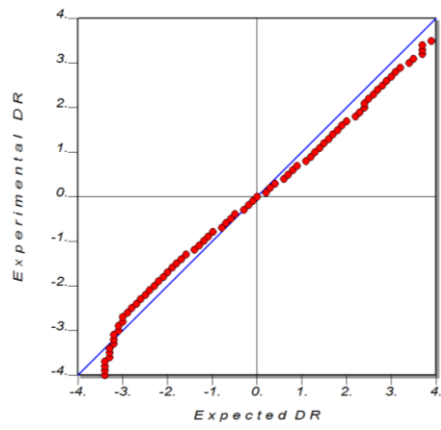
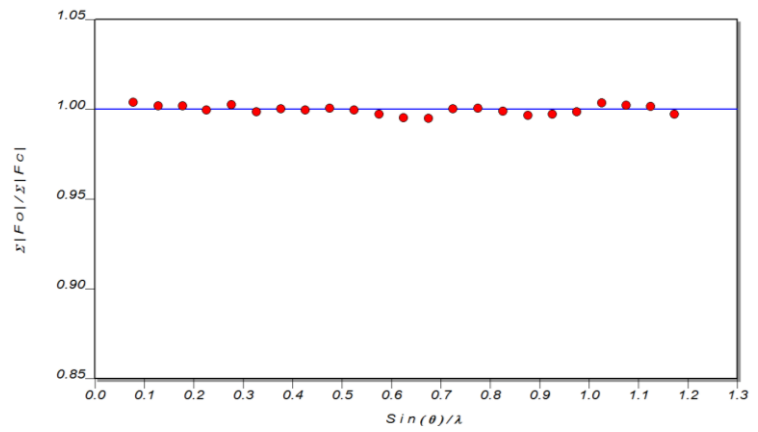


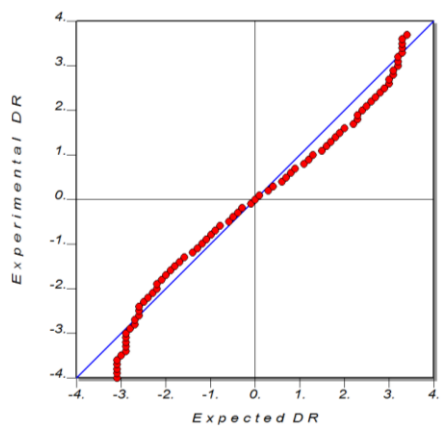
Figure 3S. Fractal plots (Meindl & Henn, 2008) for all final refinements at all temperatures: (a) 10 K, (b) 100 K, (c) 200 K, (d) 300 K. All plots are drawn based on all data.



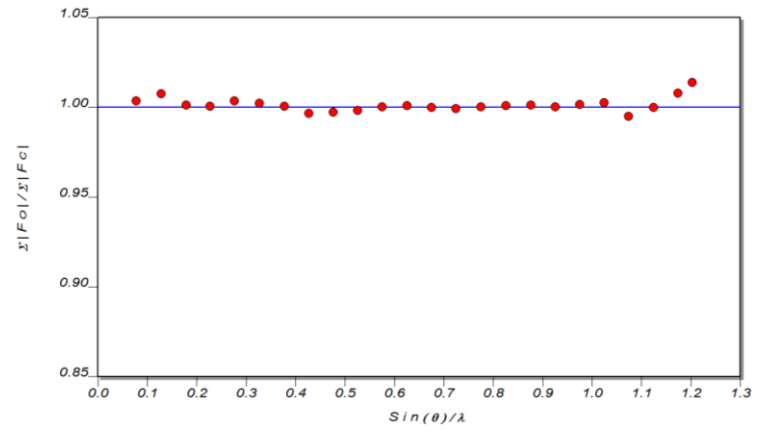
(a)



(b)



(c)



(d)

Figure 4S. Normal probability and scale plots for all final refinements at all temperatures: (a,b) 10 K, (c,d) 100 K, (e,f) 200 K, (g,h) 300 K. All plots are drawn based on all data.

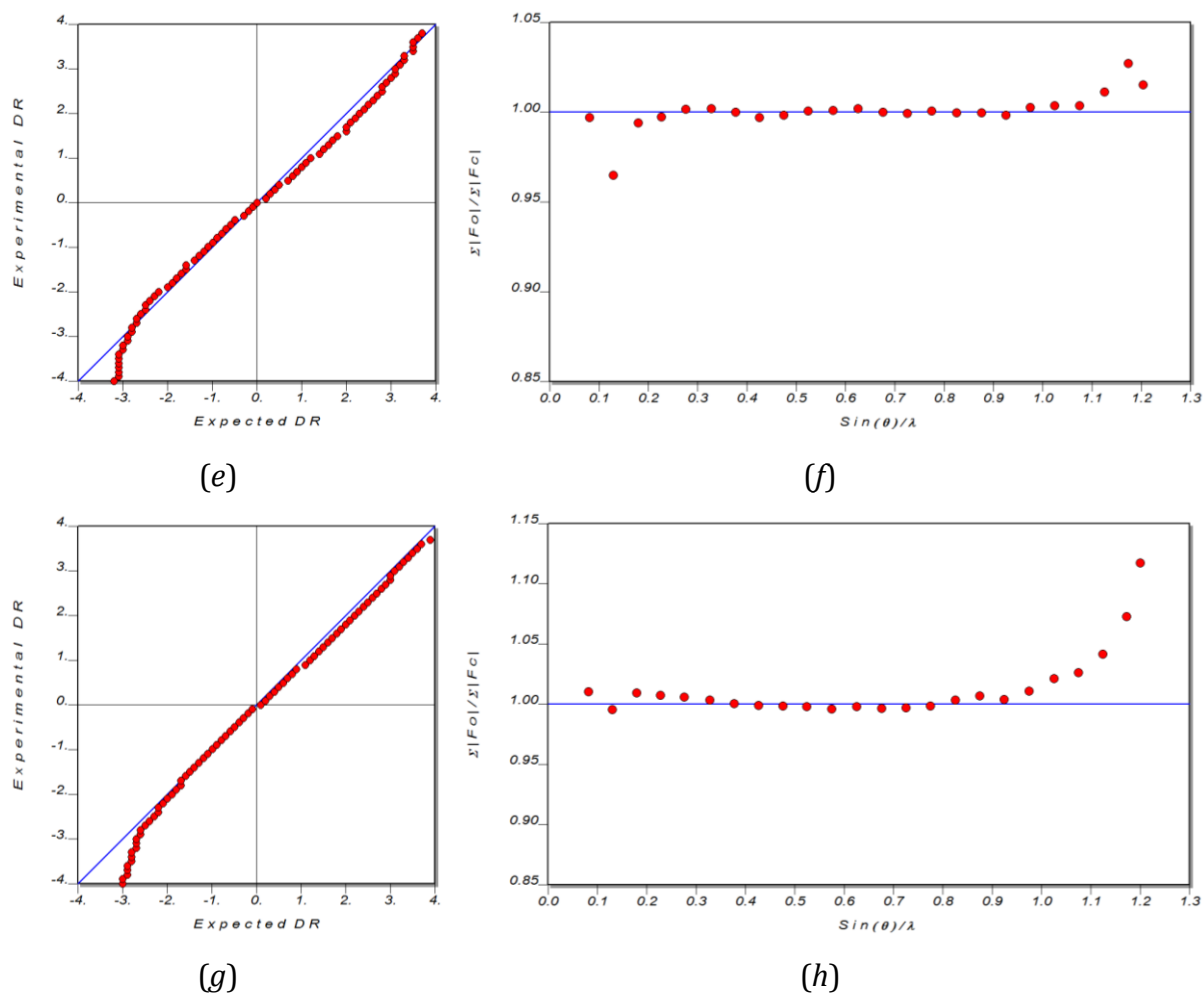


Figure 4S (continued). Normal probability and scale plots for all final refinements at all temperatures: (a,b) 10 K, (c,d) 100 K, (e,f) 200 K, (g,h) 300 K. All plots are drawn based on all data.

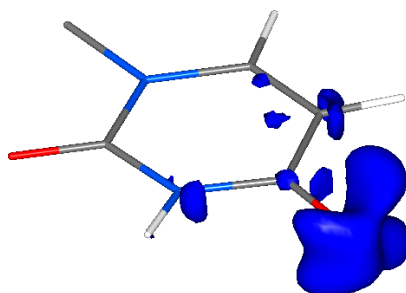


Figure 5S. Difference deformation density map ($\Delta\Delta\rho_{\text{def}} = \Delta\rho_{\text{def}}^{300\text{ K}} - \Delta\rho_{\text{def}}^{\text{UBDB}}$) in the vicinity of the O9 oxygen atom (isosurface drawn at $+0.02\text{ e}\cdot\text{\AA}^{-3}$) with reference to the UBDB-derived deformation density (all model parameters refined except for the O9 atom multipolar parameters). Spurious 'butterfly-like' pattern is clearly observed.

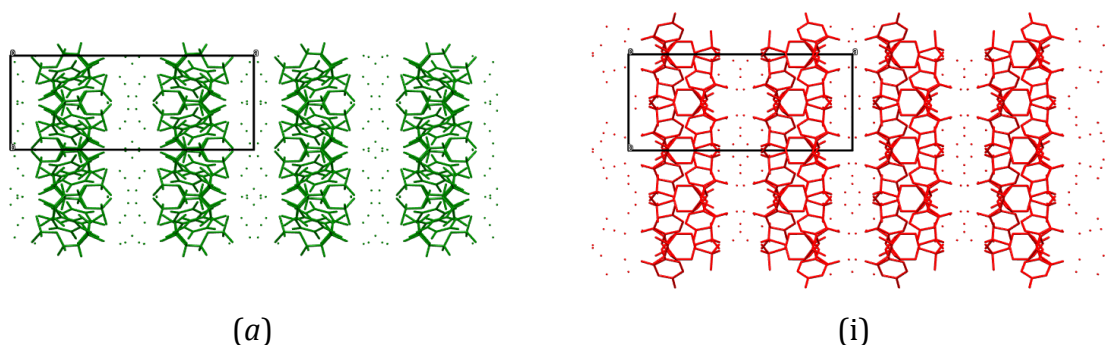


Figure 6S. Packing of sodium (a) and barium (b) uridine-5'-monophosphate hydrates. Small spheres represent water molecules. For the sodium salt the cations were not refined in the model (see the original publication). For the barium salt the cations located in-between layers were removed for clarity.

Table 2S. Bader charges (Q_{AIM}) and atomic basin volumes (V_{AIM}) for the K(UMPH) species present in the crystal lattice (data given for all data sets and for *TOPOND* results).

Atom	10 K data		100 K data		200 K data		300 K data		Theory	
	Q_{AIM}/e	$V_{\text{AIM}}/\text{\AA}^3$	Q_{AIM}/e	$V_{\text{AIM}}/\text{\AA}^3$	Q_{AIM}/e	$V_{\text{AIM}}/\text{\AA}^3$	Q_{AIM}/e	$V_{\text{AIM}}/\text{\AA}^3$	Q_{AIM}/e	$V_{\text{AIM}}/\text{\AA}^3$
K1	0.70	21.53	0.70	21.55	0.59	21.82	0.64	22.23	0.92	20.43
P1	2.91	6.81	2.90	6.81	2.99	6.32	2.68	6.24	3.77	3.25
O1	-1.16	13.71	-1.16	13.73	-1.15	13.79	-1.17	14.11	-1.30	14.37
O5	-0.95	12.72	-0.95	12.72	-0.90	12.76	-1.07	12.99	-0.96	12.96
O7	-1.02	17.25	-1.02	17.29	-0.97	16.86	-1.09	17.33	-1.10	17.39
O4	-1.29	17.44	-1.29	17.43	-1.19	17.30	-1.35	17.91	-1.45	18.39
O8	-1.07	19.25	-1.07	19.26	-1.19	19.92	-1.08	19.70	-1.15	20.13
O2	-1.32	17.55	-1.32	17.59	-1.40	18.04	-1.33	18.34	-1.52	18.76
O6	-1.08	16.78	-1.08	16.78	-1.14	17.15	-1.26	17.60	-1.12	17.53
N1	-0.98	11.33	-0.97	11.33	-0.92	11.66	-0.95	11.91	-1.06	11.39
O9	-1.09	19.65	-1.09	19.67	-0.97	19.34	-0.92	19.03	-1.16	20.57
O3	-1.29	17.48	-1.29	17.49	-1.35	17.42	-1.31	17.85	-1.53	18.77
C3	0.27	6.45	0.28	6.45	0.48	6.05	0.49	6.01	0.48	5.99
N2	-1.02	15.02	-1.02	15.02	-1.01	14.95	-1.07	15.60	-1.10	15.50
C1	0.24	8.67	0.24	8.68	0.46	7.87	0.46	8.05	0.44	7.57
C2	0.53	6.24	0.53	6.25	0.48	6.15	0.44	6.34	0.41	6.31
C6	1.60	5.26	1.59	5.28	1.64	5.26	1.52	5.48	1.64	5.16
C7	1.37	7.02	1.37	7.00	1.36	7.22	1.44	7.35	1.23	6.90
C5	0.65	5.80	0.65	5.80	0.62	5.85	0.70	5.78	0.72	5.54
C4	0.47	6.54	0.47	6.55	0.40	6.61	0.34	6.75	0.46	6.26
C9	0.08	12.83	0.07	12.85	-0.07	12.65	0.09	12.45	0.36	10.84
C8	0.19	11.97	0.19	11.99	-0.09	14.65	-0.17	15.11	0.03	12.56
H3	0.08	7.12	0.08	7.11	0.10	6.99	0.11	7.13	0.03	6.97
H1A	0.08	6.98	0.08	6.98	0.02	7.20	0.03	7.22	0.04	7.69
H1B	0.14	6.23	0.14	6.23	0.02	6.89	0.07	6.49	0.05	6.69
H2	0.04	5.88	0.04	5.88	0.06	6.09	0.19	6.25	0.06	5.87
H5	0.13	7.02	0.13	7.02	0.14	7.01	0.20	6.92	0.09	6.43
H4	0.11	6.98	0.11	7.00	0.08	7.07	0.06	7.61	0.04	7.00
H9	0.19	5.24	0.19	5.27	0.23	5.57	0.35	4.84	0.15	5.68
H8	0.16	5.81	0.16	5.82	0.30	5.45	0.41	4.58	0.08	6.56
H11	0.63	1.32	0.63	1.31	0.62	1.23	0.66	1.03	0.65	1.32
H13	0.60	1.67	0.60	1.66	0.59	1.69	0.62	1.53	0.63	1.51
H10	0.49	2.54	0.49	2.58	0.55	2.13	0.61	1.77	0.52	2.38
H12	0.63	1.50	0.63	1.51	0.62	1.70	0.66	1.39	0.63	1.60

Table 3S. Selected QTAIM parameters at BCPs for interactions in the K(UMPH) species in the crystal lattice (Atom1 & Atom2 – interacting atoms, sym2 – symmetry of the 2nd atom given as an ORTEP code, Gcp & Vcp – kinetic and potential energy densities in BCPs, DISTIJ – distance between interacting atoms; DCPI & DCPJ – distances from 1st and 2nd atom to the bond critical point, respectively, DEN – electron density, LAPL – Laplacian of electron density, ELLIPTI – bond ellipticity; all values with units as in the manuscript text).

10 K data set

Atom1	Atom2	sym2	Gcp	Vcp	DISTIJ	DCPI	DCPJ	DEN	LAPL	ELLIPTI
K1	O4	55501	25.59	-17.67	2.9253	1.4989	1.4300	0.0646	1.23	0.0327
K1	O2	55501	27.68	-19.43	2.9008	1.4836	1.4201	0.0701	1.32	0.0123
P1	O1	55501	553.03	-886.25	1.6017	0.6719	0.9340	1.1702	8.07	0.1554
P1	O4	55501	694.44	-1011.02	1.5575	0.6518	0.9084	1.2314	13.87	0.2651
P1	O2	55501	874.78	-1219.81	1.5132	0.6358	0.8780	1.3591	19.45	0.1623
P1	O3	55501	999.68	-1358.18	1.4970	0.6246	0.8735	1.4367	23.54	0.1007
O1	C1	55501	465.38	-1354.76	1.4318	0.8746	0.5576	1.6873	-15.57	0.1260
O5	C2	55501	518.17	-1346.78	1.4459	0.8580	0.5885	1.6561	-11.40	0.0641
O5	C5	55501	655.74	-1675.34	1.4149	0.8267	0.5888	1.8832	-13.36	0.0312
O7	C4	55501	492.13	-1508.41	1.4129	0.8609	0.5523	1.8108	-19.24	0.0858
O7	H13	55501	519.94	-2059.24	0.9900	0.7510	0.2390	2.2399	-37.43	0.0503
O4	H11	55501	297.07	-1695.51	1.0140	0.7922	0.2218	2.0458	-40.44	0.0043
O8	C6	55501	1315.66	-3545.53	1.2272	0.7955	0.4317	2.9751	-33.57	0.0584
O6	C3	55501	603.99	-1604.15	1.4062	0.8488	0.5575	1.8449	-14.55	0.0466
O6	H12	55501	380.58	-2178.93	0.9710	0.7497	0.2213	2.3785	-52.05	0.0002
N1	C6	55501	823.65	-2262.96	1.3847	0.8011	0.5837	2.2784	-22.60	0.2074
N1	C5	55501	541.39	-1421.00	1.4728	0.8552	0.6177	1.7126	-12.42	0.0440
N1	C9	55501	736.45	-2030.76	1.3735	0.8177	0.5559	2.1362	-20.48	0.1651
O9	C7	55501	1246.31	-3136.82	1.2358	0.8146	0.4217	2.7375	-23.65	0.0368
C3	C2	55501	548.10	-1532.69	1.5303	0.7844	0.7463	1.8076	-16.03	0.0954
C3	C4	55501	539.57	-1528.10	1.5343	0.7865	0.7500	1.8074	-16.48	0.0747
C3	H3	55501	487.74	-1537.27	1.0950	0.7305	0.3646	1.8374	-20.63	0.0501
N2	C6	55501	805.15	-2246.50	1.3716	0.7744	0.5975	2.2731	-23.36	0.1729
N2	C7	55501	630.72	-1834.86	1.3903	0.8503	0.5401	2.0239	-21.05	0.2296
N2	H10	55501	564.81	-1947.26	1.0410	0.7753	0.2657	2.1380	-30.02	0.0651
C1	C2	55501	579.64	-1632.43	1.5069	0.7889	0.7195	1.8791	-17.37	0.0976
C1	H1A	55501	548.69	-1721.40	1.0970	0.7021	0.3955	1.9655	-22.91	0.0558
C1	H1B	55501	495.22	-1660.43	1.1020	0.7211	0.3817	1.9374	-24.60	0.0437
C2	H2	55501	524.95	-1742.50	1.0930	0.6735	0.4201	1.9922	-25.43	0.0535
C7	C8	55501	692.64	-1907.46	1.4437	0.7920	0.6518	2.0570	-19.17	0.3141
C5	C4	55501	498.52	-1407.89	1.5396	0.7718	0.7679	1.7200	-15.08	0.1499
C5	H5	55501	507.41	-1685.39	1.1000	0.7605	0.3399	1.9529	-24.62	0.0531
C4	H4	55501	499.35	-1714.21	1.0880	0.7371	0.3509	1.9797	-26.27	0.0167
C9	C8	55501	807.42	-2230.22	1.3521	0.7464	0.6058	2.2602	-22.59	0.2712
C9	H9	55501	530.81	-1735.40	1.0730	0.7206	0.3525	1.9841	-24.74	0.0006
C8	H8	55501	495.29	-1663.02	1.0710	0.6603	0.4108	1.9395	-24.69	0.1514
K1	O5	45604	40.22	-29.49	2.7260	1.4177	1.3084	0.0956	1.87	0.0201
K1	O8	55502	32.56	-22.96	2.8008	1.4543	1.3466	0.0780	1.55	0.0019
K1	O9	56501	41.33	-30.45	2.7278	1.4134	1.3146	0.0981	1.92	0.0084
K1	O7	55502	34.60	-24.58	2.8040	1.4446	1.3595	0.0821	1.64	0.0350
K1	O6	55604	39.79	-28.85	2.7480	1.4204	1.3276	0.0929	1.86	0.0179
O3	C9	45604	9.51	-6.30	3.3154	1.6007	1.7188	0.0324	0.47	0.3749
O4	H1A	45604	15.75	-10.39	2.6143	1.5129	1.1416	0.0433	0.78	0.4377
O3	H13	55503	101.88	-101.40	1.6688	1.1373	0.5316	0.2624	3.76	0.0503
O2	H10	56501	94.84	-96.90	1.7240	1.1457	0.5785	0.2593	3.41	0.0067
O3	H12	55503	63.94	-95.82	1.7554	1.1492	0.6069	0.3022	1.18	0.0313
H1A	H5	65503	6.79	-4.29	2.4179	1.1881	1.2462	0.0234	0.34	0.6752
H2	H8	55402	12.97	-12.36	1.9824	1.0723	0.9235	0.0722	0.50	0.1907

O7	O4	55402	10.82	-6.90	3.1404	1.5681	1.5728	0.0316	0.54	0.0035
H13	O3	54503	101.88	-101.40	1.6688	0.5316	1.1373	0.2624	3.76	0.0638
O7	H8	55402	6.12	-4.47	2.7661	1.6240	1.1720	0.0307	0.28	0.2321
O4	O7	55502	10.82	-6.90	3.1404	1.5728	1.5681	0.0316	0.54	0.0077
H11	O2	45604	126.38	-224.59	1.5425	0.5059	1.0366	0.5271	1.03	0.0150
O8	O6	54503	10.12	-6.40	3.1577	1.5744	1.5852	0.0298	0.51	0.3605
C6	C8	54604	5.60	-3.92	3.5223	1.7908	1.7640	0.0266	0.27	0.5713
O8	H2	64503	7.76	-5.44	2.7364	1.5636	1.2317	0.0326	0.37	0.1873
O2	H11	55604	126.38	-224.59	1.5425	1.0366	0.5059	0.5271	1.03	0.0140
O6	O8	55503	10.12	-6.40	3.1577	1.5852	1.5744	0.0298	0.51	0.3621
H12	O3	54503	63.94	-95.82	1.7554	0.6069	1.1492	0.3022	1.18	0.0278
O6	H4	55503	12.35	-10.10	2.6556	1.4758	1.1917	0.0567	0.54	0.0097
O6	H1B	54503	5.59	-4.02	3.0501	1.7166	1.3932	0.0282	0.26	0.4556
N1	O9	54604	7.06	-4.74	3.3753	1.7591	1.7093	0.0280	0.34	2.0314
C9	O3	55604	9.51	-6.30	3.3154	1.7188	1.6007	0.0324	0.47	0.3654
H5	H1A	64503	6.79	-4.29	2.4179	1.2462	1.1882	0.0234	0.34	0.6754
O9	N1	44604	7.06	-4.74	3.3753	1.7093	1.7591	0.0280	0.34	2.0314
O9	H3	54604	4.79	-2.85	3.1271	1.7262	1.4072	0.0155	0.25	0.2748
O9	H5	44604	8.46	-5.25	2.8845	1.6001	1.2916	0.0253	0.43	0.3502
O9	H1B	55502	5.32	-3.40	2.8761	1.6525	1.3077	0.0208	0.27	0.0847
O9	H2	55502	5.74	-3.49	2.9561	1.6692	1.3289	0.0187	0.29	0.1407
O5	K1	55604	40.22	-29.49	2.7260	1.3084	1.4177	0.0956	1.87	0.0179
H4	O6	54503	12.35	-10.10	2.6556	1.1917	1.4758	0.0567	0.54	0.0121
H3	O9	44604	4.79	-2.85	3.1271	1.4072	1.7262	0.0155	0.25	0.0495
O8	K1	55402	32.56	-22.95	2.8008	1.3466	1.4543	0.0780	1.55	0.0056
H10	O2	54501	94.84	-96.90	1.7240	0.5785	1.1457	0.2593	3.41	0.0067
H1A	O4	55604	15.75	-10.39	2.6143	1.1416	1.5129	0.0433	0.78	0.4383
H1B	H4	55503	8.11	-5.90	2.4509	1.2741	1.1926	0.0360	0.38	1.3666
H2	O8	65503	7.76	-5.44	2.7364	1.2317	1.5636	0.0326	0.37	0.1725
O9	K1	54501	41.33	-30.45	2.7278	1.3146	1.4134	0.0981	1.92	0.0078
H8	O7	55502	6.12	-4.47	2.7661	1.1720	1.6240	0.0307	0.28	0.2410
H4	H1B	54503	8.11	-5.90	2.4509	1.1926	1.2741	0.0360	0.38	1.3665
H5	O9	54604	8.46	-5.25	2.8845	1.2916	1.6001	0.0253	0.43	0.3524
C8	C6	44604	5.60	-3.92	3.5223	1.7639	1.7907	0.0266	0.27	0.5711
H8	H2	55502	12.97	-12.36	1.9824	0.9235	1.0723	0.0722	0.50	0.1907
H1B	O6	55503	5.59	-4.02	3.0501	1.3932	1.7167	0.0282	0.26	0.4561
H1B	O9	55402	5.32	-3.40	2.8761	1.3077	1.6524	0.0208	0.27	0.0846
H2	O9	55402	5.74	-3.49	2.9561	1.3289	1.6692	0.0187	0.29	0.1786
O2	H10	44604	94.84	-96.90	1.7240	1.1457	0.5786	0.2593	3.41	0.0267
O7	K1	55402	34.60	-24.58	2.8040	1.3595	1.4446	0.0821	1.64	0.0194
O6	K1	45604	39.80	-28.85	2.7480	1.3276	1.4204	0.0930	1.86	0.0446
O1	H9	55501	17.89	-15.36	2.3956	1.4181	0.9826	0.0761	0.75	0.0096

100 K data set

Atom1	Atom2	sym2	Gcp	Vcp	DISTIJ	DCPI	DCPJ	DEN	LAPL	ELLIPTI
K1	O4	55501	25.78	-17.87	2.9197	1.5005	1.4230	0.0654	1.24	0.0427
K1	O2	55501	27.30	-19.13	2.9083	1.4894	1.4224	0.0693	1.30	0.1163
P1	O1	55501	517.29	-869.76	1.6008	0.6709	0.9337	1.1718	6.05	0.4029
P1	O4	55501	684.19	-1015.67	1.5557	0.6487	0.9079	1.2422	12.95	0.3359
P1	O2	55501	904.11	-1260.25	1.5108	0.6336	0.8788	1.3857	20.12	0.1731
P1	O3	55501	975.56	-1336.95	1.4952	0.6275	0.8691	1.4275	22.55	0.2201
O1	C1	55501	562.61	-1462.27	1.4300	0.8506	0.5803	1.7399	-12.37	0.0810
O5	C2	55501	509.69	-1370.25	1.4448	0.8553	0.5896	1.6813	-12.88	0.1374
O5	C5	55501	527.74	-1557.05	1.4145	0.8579	0.5570	1.8372	-18.41	0.0796
O7	C4	55501	593.61	-1626.30	1.4111	0.8390	0.5726	1.8680	-16.12	0.0282
O7	H13	55501	476.63	-2412.41	0.9700	0.7466	0.2234	2.5092	-53.57	0.0007
O4	H11	55501	266.34	-1777.31	1.0150	0.7886	0.2264	2.1220	-45.70	0.0142
O8	C6	55501	1417.61	-3497.69	1.2261	0.8087	0.4174	2.9136	-24.32	0.1282
O6	C3	55501	617.07	-1670.81	1.4049	0.8509	0.5541	1.8955	-16.03	0.0654
O6	H12	55501	393.53	-2028.44	0.9699	0.7574	0.2126	2.2640	-45.58	0.0353
N1	C6	55501	757.50	-2128.60	1.3846	0.7991	0.5859	2.2028	-22.53	0.2148
N1	C5	55501	552.15	-1554.96	1.4711	0.8432	0.6280	1.8250	-16.55	0.1141
N1	C9	55501	784.43	-2196.31	1.3698	0.7993	0.5708	2.2435	-23.04	0.1679
O9	C7	55501	1443.54	-3209.91	1.2333	0.8270	0.4064	2.7208	-11.85	0.0764
C3	C2	55501	562.52	-1564.51	1.5290	0.7753	0.7540	1.8288	-16.13	0.1696
C3	C4	55501	528.76	-1474.96	1.5322	0.7940	0.7395	1.7659	-15.33	0.0517

C3	H3	55501	487.93-1607.93	1.0980	0.7188	0.3796	1.8970-23.21-	0.0328
N2	C6	55501	798.30-2208.34	1.3698	0.7767	0.5936	2.2473-22.46-	0.1800
N2	C7	55501	609.69-1933.93	1.3847	0.8434	0.5418	2.1103-26.23-	0.1193
N2	H10	55501	508.38-2143.03	1.0300	0.7568	0.2734	2.3062-41.35-	0.0397
C1	C2	55501	583.85-1607.90	1.5057	0.7653	0.7405	1.8566-16.16-	0.1086
C1	H1A	55501	565.55-1809.32	1.0910	0.6959	0.3952	2.0295-24.90-	0.0517
C1	H1B	55501	486.98-1593.83	1.0910	0.7221	0.3692	1.8856-22.76-	0.0397
C2	H2	55501	507.58-1707.09	1.0980	0.6797	0.4184	1.9705-25.40-	0.0909
C7	C8	55501	661.48-1819.69	1.4398	0.7845	0.6555	1.9994-18.24-	0.2536
C5	C4	55501	532.20-1495.67	1.5381	0.8000	0.7383	1.7825-15.83-	0.0478
C5	H5	55501	536.12-1796.55	1.0981	0.7445	0.3536	2.0311-26.59-	0.0016
C4	H4	55501	502.85-1706.32	1.0979	0.7204	0.3775	1.9718-25.72-	0.0328
C9	C8	55501	836.85-2302.38	1.3508	0.6962	0.6550	2.3026-23.08-	0.2375
C9	H9	55501	509.49-1707.95	1.0830	0.7505	0.3327	1.9705-25.30-	0.0391
C8	H8	55501	490.10-1485.07	1.0831	0.7068	0.3763	1.7916-18.54-	0.1069
K1	O5	45604	40.90 -30.11	2.7282	1.4175	1.3107	0.0973 1.90	0.0292
K1	O8	55502	32.35 -22.77	2.7999	1.4587	1.3412	0.0774 1.54	0.0029
K1	O9	56501	41.33 -30.30	2.7217	1.4167	1.3051	0.0972 1.92	0.0007
K1	O7	55502	34.42 -24.47	2.8025	1.4479	1.3546	0.0820 1.63	0.0238
K1	O6	55604	40.16 -29.06	2.7453	1.4219	1.3234	0.0931 1.88	0.0212
O3	C9	45604	9.96 -6.80	3.3215	1.5853	1.7498	0.0358 0.48	0.4492
O3	H13	55503	88.31 -106.08	1.6828	1.1326	0.5504	0.2967 2.59	0.0149
O2	H10	56501	67.21 -95.36	1.7386	1.1501	0.5892	0.2962 1.43	0.0093
O3	H12	55503	75.64 -79.02	1.7533	1.1739	0.5794	0.2324 2.65	0.0022
H1A	H5	65503	7.65 -5.08	2.4025	1.1305	1.2766	0.0287 0.37	1.0322
H2	H8	55402	15.55 -12.79	1.9576	1.0687	0.9305	0.0657 0.67	0.1503
O7	O4	55402	10.67 -6.79	3.1390	1.5646	1.5751	0.0312 0.53	0.0126
H13	O3	54503	88.31 -106.08	1.6828	0.5504	1.1326	0.2967 2.59	0.0091
O7	H8	55402	7.12 -4.14	2.7977	1.7103	1.1629	0.0180 0.37	0.7748
O4	O7	55502	10.67 -6.79	3.1390	1.5751	1.5646	0.0312 0.53	0.0087
H11	O2	45604	114.10 -227.46	1.5379	0.4961	1.0420	0.5446 0.03	0.0044
O8	O6	54503	10.25 -6.49	3.1589	1.5749	1.5864	0.0301 0.51	0.2515
O8	C8	54604	5.65 -3.89	3.7199	1.9265	1.8468	0.0260 0.27	1.2204
O8	H2	64503	8.06 -5.55	2.7328	1.5702	1.2164	0.0321 0.39	0.2579
O2	H11	55604	114.10 -227.46	1.5379	1.0420	0.4961	0.5446 0.03	0.0075
O2	H3	55604	1.83 -1.07	3.5829	1.9184	1.6737	0.0081 0.10	0.7197
O6	O8	55503	10.25 -6.49	3.1589	1.5864	1.5749	0.0301 0.51	0.2584
H12	O3	54503	75.64 -79.02	1.7533	0.5794	1.1739	0.2324 2.65	0.0011
O6	H4	55503	11.20 -9.18	2.6648	1.4902	1.1909	0.0537 0.49	0.0331
O6	H1B	54503	5.47 -3.79	3.0956	1.7474	1.3854	0.0259 0.26	0.1119
N1	O9	54604	7.45 -4.84	3.4102	1.7781	1.6795	0.0267 0.37	2.7275
C9	O3	55604	9.96 -6.80	3.3215	1.7498	1.5853	0.0358 0.48	0.4483
H5	H1A	64503	7.65 -5.08	2.4025	1.2766	1.1305	0.0287 0.37	1.0322
O9	N1	44604	7.45 -4.84	3.4102	1.6795	1.7781	0.0267 0.37	2.7274
O9	H3	54604	4.86 -2.88	3.0711	1.7217	1.3553	0.0154 0.25	0.6250
O9	H1B	55502	5.98 -3.75	2.8964	1.6374	1.2990	0.0211 0.30	0.2742
O5	K1	55604	40.90 -30.11	2.7282	1.3107	1.4175	0.0973 1.90	0.0332
H4	O6	54503	11.20 -9.18	2.6648	1.1909	1.4902	0.0537 0.49	0.0225
H3	O9	44604	4.86 -2.88	3.0711	1.3553	1.7217	0.0154 0.25	0.6223
O8	K1	55402	32.34 -22.77	2.7999	1.3412	1.4587	0.0774 1.54	0.0001
H10	O2	54501	67.21 -95.36	1.7386	0.5892	1.1501	0.2962 1.43	0.0093
H1B	H4	55503	7.99 -5.71	2.4384	1.2754	1.1721	0.0345 0.38	1.1761
H2	O8	65503	8.06 -5.55	2.7328	1.2164	1.5702	0.0321 0.39	0.2588
O9	K1	54501	41.33 -30.30	2.7217	1.3051	1.4167	0.0972 1.92	0.0012
H8	O7	55502	7.12 -4.14	2.7977	1.1629	1.7103	0.0180 0.37	0.7746
H4	H1B	54503	7.99 -5.71	2.4384	1.1721	1.2754	0.0345 0.38	1.1761
C8	O8	44604	5.65 -3.89	3.7199	1.8468	1.9265	0.0260 0.27	1.2202
H8	H2	55502	15.55 -12.79	1.9576	0.9305	1.0687	0.0657 0.67	0.1465
H3	O2	45604	1.83 -1.07	3.5829	1.6737	1.9184	0.0081 0.10	0.7194
H1B	O6	55503	5.47 -3.79	3.0956	1.3854	1.7474	0.0259 0.26	0.0922
H1B	O9	55402	5.98 -3.75	2.8964	1.2990	1.6374	0.0211 0.30	0.2759
O2	H10	44604	67.21 -95.36	1.7386	1.1501	0.5892	0.2962 1.43	0.0091
O7	K1	55402	34.42 -24.47	2.8025	1.3546	1.4479	0.0820 1.63	0.0138
O6	K1	45604	40.16 -29.06	2.7453	1.3234	1.4219	0.0932 1.88	0.0123
O1	H9	55501	16.89 -11.76	2.4305	1.4725	0.9614	0.0512 0.81	0.0541

200 K data set

Atom1	Atom2	sym2	Gcp	Vcp	DISTIJ	DCPI	DCPJ	DEN	LAPL	ELLIPTI
K1	O4	55501	25.90	-17.81	2.9200	1.4996	1.4232	0.0644	1.25	0.0073
K1	O2	55501	26.31	-18.26	2.9283	1.4951	1.4357	0.0664	1.26	0.0748
P1	O1	55501	588.23	-848.11	1.5998	0.6684	0.9322	1.1048	12.06	0.4657
P1	O4	55501	727.34	-936.39	1.5557	0.6490	0.9068	1.1270	19.03	0.2868
P1	O2	55501	928.12	-1300.24	1.5108	0.6338	0.8773	1.4143	20.41	0.0486
P1	O3	55501	1010.90	-1395.33	1.4949	0.6268	0.8682	1.4682	23.00	-0.1042
O1	C1	55501	537.02	-1510.28	1.4290	0.8469	0.5838	1.7931	-16.02	-0.0921
O5	C2	55501	545.61	-1453.81	1.4445	0.8473	0.5973	1.7399	-13.31	-0.1704
O5	C5	55501	574.04	-1499.01	1.4139	0.8458	0.5682	1.7672	-12.88	-0.2591
O7	C4	55501	539.81	-1479.68	1.4117	0.8538	0.5584	1.7652	-14.69	-0.0272
O7	H13	55501	510.51	-2119.73	0.9700	0.7460	0.2239	2.2883	-40.34	-0.0121
O4	H11	55501	394.98	-2130.47	1.0150	0.7808	0.2343	2.3384	-49.22	-0.0008
O8	C6	55501	1338.50	-3309.34	1.2271	0.8027	0.4248	2.8193	-23.22	-0.0405
O6	C3	55501	616.97	-1645.15	1.4055	0.8670	0.5385	1.8741	-15.10	-0.0885
O6	H12	55501	435.34	-2017.97	0.9699	0.7542	0.2158	2.2407	-42.12	-0.0493
N1	C6	55501	796.77	-2187.65	1.3830	0.7925	0.5912	2.2324	-21.81	-0.2992
N1	C5	55501	569.04	-1503.45	1.4721	0.8520	0.6204	1.7732	-13.41	-0.2149
N1	C9	55501	782.62	-2105.42	1.3653	0.7853	0.5804	2.1757	-19.83	-0.2766
O9	C7	55501	1285.53	-3070.40	1.2363	0.8148	0.4217	2.6809	-18.33	-0.1748
C3	C2	55501	532.38	-1464.63	1.5269	0.7692	0.7581	1.7553	-14.68	-0.1471
C3	C4	55501	519.35	-1426.89	1.5316	0.7761	0.7578	1.7277	-14.25	-0.0229
C3	H3	55501	465.62	-1577.24	1.0980	0.7263	0.3718	1.8806	-23.72	-0.0011
N2	C6	55501	801.43	-2258.60	1.3704	0.7830	0.5885	2.2834	-24.08	-0.1932
N2	C7	55501	643.88	-1895.24	1.3820	0.8362	0.5466	2.0666	-22.30	-0.0609
N2	H10	55501	485.28	-1959.18	1.0300	0.7744	0.2560	2.1775	-36.30	-0.0504
C1	C2	55501	562.44	-1463.63	1.5045	0.7595	0.7451	1.7411	-12.44	-0.1428
C1	H1A	55501	577.83	-1876.53	1.0910	0.6653	0.4260	2.0779	-26.47	-0.0864
C1	H1B	55501	521.36	-1668.76	1.0910	0.6862	0.4056	1.9335	-22.99	-0.0854
C2	H2	55501	497.95	-1625.80	1.0980	0.6850	0.4133	1.9077	-23.13	-0.0513
C7	C8	55501	642.14	-1821.94	1.4330	0.7442	0.6890	2.0090	-19.74	-0.3234
C5	C4	55501	530.39	-1416.03	1.5374	0.7835	0.7543	1.7131	-13.04	-0.0671
C5	H5	55501	523.53	-1736.00	1.0980	0.7513	0.3467	1.9875	-25.29	-0.0143
C4	H4	55501	523.60	-1637.03	1.0980	0.7354	0.3630	1.9063	-21.66	-0.0108
C9	C8	55501	856.42	-2312.07	1.3487	0.7607	0.5889	2.3025	-22.00	-0.4315
C9	H9	55501	511.16	-1481.06	1.0829	0.7719	0.3117	1.7789	-16.84	-0.1486
C8	H8	55501	480.26	-1287.65	1.0830	0.7207	0.3638	1.6191	-12.01	-0.2888
K1	O5	45604	39.29	-28.64	2.7411	1.4249	1.3162	0.0932	1.83	0.0100
K1	O8	55502	32.90	-23.27	2.8057	1.4550	1.3507	0.0789	1.56	0.0075
K1	O9	56501	41.47	-30.17	2.7137	1.4168	1.2969	0.0960	1.94	0.0137
K1	O7	55502	34.29	-24.35	2.8028	1.4488	1.3541	0.0816	1.62	0.0161
K1	O6	55604	39.02	-28.18	2.7541	1.4269	1.3273	0.0912	1.83	0.0029
O4	O7	55502	10.20	-6.51	3.1496	1.5816	1.5684	0.0307	0.51	0.0006
O3	C9	45604	11.10	-8.25	3.3446	1.5562	1.8055	0.0453	0.51	0.6945
O4	H1A	45604	12.41	-7.81	2.6434	1.5620	1.0903	0.0331	0.62	1.5954
O3	H13	55503	96.44	-123.02	1.6883	1.1145	0.5745	0.3323	2.56	0.0285
O2	H10	56501	83.74	-84.61	1.7436	1.1740	0.5697	0.2375	3.04	0.0017
O3	H12	55503	77.47	-85.41	1.7553	1.1674	0.5880	0.2504	2.55	0.0130
H1A	H5	65503	5.70	-3.97	2.3942	1.1707	1.2507	0.0268	0.27	0.5430
H2	H8	55402	11.93	-8.76	1.9910	1.0360	1.0478	0.0463	0.55	1.0192
O7	O4	55402	10.20	-6.51	3.1496	1.5684	1.5816	0.0307	0.51	0.0012
H13	O3	54503	96.44	-123.02	1.6883	0.5745	1.1145	0.3323	2.56	0.0046
H11	O2	45604	121.84	-216.14	1.5413	0.4903	1.0512	0.5149	1.01	0.0042
O8	O6	54503	9.99	-6.29	3.1665	1.5724	1.5952	0.0291	0.50	0.3358
O8	H2	64503	9.03	-5.62	2.7656	1.5859	1.1798	0.0265	0.46	0.5043
C6	C8	54604	5.24	-3.93	3.6442	1.7847	1.9313	0.0294	0.24	0.1980
O2	H11	55604	121.84	-216.14	1.5413	1.0512	0.4903	0.5149	1.01	0.0146
O2	H3	55604	1.87	-1.10	3.6121	1.9266	1.6975	0.0084	0.10	0.6474
O6	O8	55503	9.99	-6.29	3.1665	1.5952	1.5724	0.0291	0.50	0.3356
H12	O3	54503	77.47	-85.41	1.7553	0.5880	1.1674	0.2504	2.55	0.0110
O6	H4	55503	10.03	-7.01	2.7068	1.5436	1.1639	0.0377	0.48	0.0596
O6	C8	55402	6.42	-4.19	3.7819	1.7460	2.0613	0.0246	0.32	1.7133
O6	H1B	54503	4.87	-3.30	3.1327	1.7885	1.3950	0.0228	0.24	1.3897
N1	O9	54604	6.24	-3.89	3.4581	1.8076	1.6756	0.0213	0.32	0.9472
C9	O3	55604	11.10	-8.25	3.3446	1.8055	1.5562	0.0453	0.51	0.6953
H5	H1A	64503	5.70	-3.97	2.3942	1.2507	1.1707	0.0268	0.27	0.5430
O9	N1	44604	6.24	-3.89	3.4581	1.6756	1.8076	0.0213	0.32	0.9472
O9	H3	54604	5.04	-3.07	3.0169	1.6987	1.3437	0.0175	0.26	0.4655

O9	H1B	55502	5.41	-3.32	2.9104	1.6605	1.2933	0.0187	0.28	0.3419
O5	K1	55604	39.29	-28.64	2.7411	1.3162	1.4249	0.0932	1.83	0.0173
H2	O8	65503	9.03	-5.62	2.7656	1.1798	1.5859	0.0265	0.46	0.5048
H4	O6	54503	10.03	-7.01	2.7068	1.1639	1.5436	0.0377	0.48	0.0602
H3	O9	44604	5.04	-3.07	3.0169	1.3437	1.6988	0.0175	0.26	0.4645
O8	K1	55402	32.90	-23.27	2.8057	1.3507	1.4550	0.0789	1.56	0.0046
H10	O2	54501	83.74	-84.61	1.7436	0.5697	1.1740	0.2375	3.04	0.0017
H1B	H4	55503	6.98	-5.15	2.4890	1.2572	1.2597	0.0338	0.32	0.3127
O9	K1	54501	41.47	-30.17	2.7137	1.2969	1.4168	0.0960	1.94	0.0133
C8	O6	55502	6.42	-4.19	3.7819	2.0613	1.7462	0.0246	0.32	1.7248
H4	H1B	54503	6.98	-5.15	2.4890	1.2597	1.2572	0.0338	0.32	0.3211
C8	C6	44604	5.24	-3.93	3.6442	1.9313	1.7847	0.0294	0.24	0.1283
H8	H2	55502	11.93	-8.76	1.9910	1.0478	1.0360	0.0463	0.55	1.0192
H3	O2	45604	1.87	-1.10	3.6121	1.6975	1.9266	0.0084	0.10	0.6471
H1A	O4	55604	12.41	-7.81	2.6434	1.0903	1.5620	0.0331	0.62	1.5954
H1B	O6	55503	4.87	-3.30	3.1327	1.3950	1.7885	0.0228	0.24	1.3961
H1B	O9	55402	5.41	-3.32	2.9104	1.2933	1.6605	0.0186	0.28	0.3440
H1A	O4	55402	12.41	-7.81	2.6434	1.0903	1.5620	0.0331	0.62	1.5934
O2	H10	44604	83.74	-84.61	1.7436	1.1740	0.5697	0.2375	3.04	0.0147
O7	K1	55402	34.29	-24.35	2.8028	1.3541	1.4488	0.0816	1.62	0.0167
O6	K1	45604	39.02	-28.18	2.7541	1.3273	1.4269	0.0912	1.83	0.0243
O1	H9	55501	14.88	-9.67	2.4721	1.5051	1.0727	0.0403	0.74	1.3044
O5	H9	55501	45.36	-38.92	2.3073	1.2910	1.0565	0.1329	1.90	0.8647

300 K data set

Atom1	Atom2	sym2	Gcp	Vcp	DISTIJ	DCPI	DCPJ	DEN	LAPL	ELLIPTI
K1	O4	55501	26.28	-18.08	2.9237	1.4943	1.4301	0.0651	1.27	0.1011
K1	O2	55501	25.42	-17.51	2.9367	1.4989	1.4388	0.0639	1.22	0.1009
P1	O1	55501	580.38	-990.17	1.5998	0.6973	0.9039	1.2712	6.26	0.1988
P1	O4	55501	698.23	-1049.74	1.5592	0.6713	0.8901	1.2719	12.73	0.1266
P1	O2	55501	908.62	-1373.59	1.5094	0.6550	0.8568	1.4971	16.29	0.1560
P1	O3	55501	1003.79	-1492.63	1.4915	0.6454	0.8467	1.5658	18.91	0.2073
O1	C1	55501	578.96	-1523.64	1.4263	0.8276	0.6006	1.7865	-13.43	0.0964
O5	C2	55501	560.76	-1599.97	1.4433	0.8588	0.5847	1.8597	-17.57	0.0510
O5	C5	55501	673.38	-1793.98	1.4133	0.8271	0.5873	1.9738	-16.42	0.2361
O7	C4	55501	577.59	-1556.21	1.4099	0.8459	0.5652	1.8152	-14.72	0.0606
O7	H13	55501	454.11	-2102.11	0.9699	0.7447	0.2254	2.2961	-43.83	0.0141
O4	H11	55501	304.92	-2096.34	1.0150	0.7885	0.2266	2.3463	-54.58	0.0236
O8	C6	55501	1214.51	-3474.93	1.2271	0.7763	0.4512	2.9627	-38.40	0.0994
O6	C3	55501	668.01	-1806.65	1.4076	0.8635	0.5452	1.9862	-17.28	0.0333
O6	H12	55501	391.48	-2134.01	0.9699	0.7556	0.2144	2.3422	-49.60	0.0810
N1	C6	55501	843.76	-2337.50	1.3828	0.8014	0.5817	2.3257	-23.86	0.1688
N1	C5	55501	536.25	-1482.95	1.4710	0.8582	0.6138	1.7696	-15.07	0.1721
N1	C9	55501	894.44	-2301.55	1.3650	0.7601	0.6054	2.2808	-18.82	0.3447
O9	C7	55501	1341.36	-3704.62	1.2129	0.7927	0.4206	3.0646	-37.52	0.1372
C3	C2	55501	553.29	-1535.45	1.5250	0.7605	0.7653	1.8078	-15.75	0.1567
C3	C4	55501	558.08	-1544.03	1.5302	0.7590	0.7733	1.8131	-15.71	0.0402
C3	H3	55501	465.88	-1626.68	1.0980	0.6899	0.4106	1.9217	-25.51	0.0010
N2	C6	55501	906.94	-2452.23	1.3689	0.7719	0.5988	2.3858	-23.44	0.1053
N2	C7	55501	659.40	-1995.47	1.3775	0.8351	0.5434	2.1387	-24.84	0.1084
N2	H10	55501	387.82	-1994.96	1.0300	0.7833	0.2472	2.2412	-44.77	0.0109
C1	C2	55501	577.30	-1511.36	1.5050	0.7566	0.7485	1.7765	-13.10	0.1806
C1	H1A	55501	582.19	-1847.75	1.0910	0.6502	0.4412	2.0535	-25.09	0.1666
C1	H1B	55501	539.12	-1652.89	1.0911	0.6665	0.4254	1.9131	-21.10	0.1624
C2	H2	55501	428.99	-1551.20	1.0980	0.7273	0.3708	1.8741	-25.45	0.0643
C7	C8	55501	666.23	-1771.04	1.4255	0.7522	0.6736	1.9580	-16.10	0.3353
C5	C4	55501	528.18	-1476.39	1.5363	0.7533	0.7834	1.7674	-15.42	0.0195
C5	H5	55501	495.21	-1752.70	1.0981	0.7570	0.3414	2.0124	-27.99	0.0002
C4	H4	55501	526.86	-1655.35	1.0980	0.7214	0.3771	1.9202	-22.09	0.0345
C9	C8	55501	901.86	-2297.73	1.3449	0.6957	0.6494	2.2752	-18.14	0.5302
C9	H9	55501	465.10	-1453.53	1.0830	0.7679	0.3154	1.7750	-19.21	0.1680
C8	H8	55501	466.32	-1128.28	1.0830	0.7185	0.3670	1.4733	-7.18	0.6857
K1	O5	45604	38.27	-27.84	2.7557	1.4281	1.3277	0.0914	1.79	0.0313
K1	O8	55502	32.09	-22.59	2.8084	1.4581	1.3503	0.0770	1.53	0.0011
K1	O9	56501	39.58	-27.73	2.7246	1.4305	1.2943	0.0865	1.89	0.0043
K1	O7	55502	34.42	-24.45	2.8087	1.4470	1.3620	0.0818	1.63	0.0058

K1	O6	55604	37.20	-26.70	2.7656	1.4333	1.3324	0.0875	1.75	0.0061
O4	O7	55502	10.55	-6.80	3.1573	1.5892	1.5681	0.0321	0.53	0.0025
O3	H12	55503	73.50	-76.02	1.7580	1.1945	0.5637	0.2258	2.61	0.0107
O3	C9	45604	10.10	-7.17	3.3664	1.5857	1.7883	0.0392	0.48	1.2888
O3	H13	55503	92.28	-127.67	1.6883	1.1234	0.5652	0.3499	2.09	0.0095
O2	H10	56501	70.16	-76.37	1.7520	1.1888	0.5632	0.2327	2.35	0.0060
H1B	O9	55402	4.04	-2.31	2.9183	1.2383	1.7264	0.0119	0.21	0.5165
H3	O9	44604	4.36	-2.72	2.9912	1.3994	1.6850	0.0172	0.22	0.4706
H1A	H5	65503	5.04	-4.05	2.4024	1.1722	1.2728	0.0322	0.22	0.1100
H2	H8	55402	8.55	-6.58	2.0333	1.1435	1.0759	0.0411	0.39	1.2894
O7	O4	55402	10.55	-6.80	3.1573	1.5681	1.5892	0.0321	0.53	0.0091
H13	O3	54503	92.28	-127.67	1.6883	0.5652	1.1234	0.3499	2.09	0.0232
O7	H1A	64503	3.39	-2.25	3.3278	1.7383	1.5918	0.0174	0.17	1.2806
H11	O2	45604	103.15	-200.40	1.5476	0.4890	1.0595	0.5021	0.22	0.0031
O8	O6	54503	9.67	-6.09	3.1712	1.5661	1.6056	0.0286	0.49	0.2999
O8	H2	64503	7.95	-5.18	2.7684	1.5843	1.2005	0.0279	0.39	0.4671
C6	C8	54604	4.31	-3.12	3.6957	1.7632	1.9960	0.0245	0.20	0.8518
O2	H11	55604	103.15	-200.40	1.5476	1.0595	0.4890	0.5021	0.22	0.0115
O2	H3	55604	1.97	-1.19	3.6492	1.9094	1.7597	0.0096	0.10	0.2999
O4	H1A	45604	8.98	-6.09	2.6665	1.5974	1.1425	0.0330	0.44	0.5125
H12	O3	54503	73.50	-76.02	1.7580	0.5637	1.1945	0.2258	2.61	0.0012
O6	O8	55503	9.67	-6.09	3.1712	1.6056	1.5661	0.0286	0.49	0.3007
O6	H4	55503	9.70	-7.29	2.7387	1.5328	1.2174	0.0426	0.44	0.0211
O6	C8	55402	6.63	-4.37	3.7811	1.7149	2.0841	0.0258	0.33	1.4019
N1	O9	54604	5.34	-3.17	3.4964	1.8602	1.6410	0.0164	0.28	0.5154
C9	O3	55604	10.10	-7.17	3.3664	1.7883	1.5857	0.0392	0.48	1.2888
C9	N2	44604	1.61	-0.91	4.0511	2.0997	2.1250	0.0065	0.08	1.0523
O9	H1B	55502	4.04	-2.31	2.9183	1.7265	1.2383	0.0119	0.21	0.5138
O9	N1	44604	5.34	-3.17	3.4964	1.6410	1.8602	0.0164	0.28	0.5156
O9	H3	54604	4.36	-2.72	2.9912	1.6850	1.3994	0.0172	0.22	0.4706
O9	H4	54604	2.48	-1.41	3.2831	1.8119	1.5319	0.0086	0.13	0.6518
O3	C8	45604	9.96	-7.21	3.4017	1.5785	1.8345	0.0404	0.47	1.1255
O5	K1	55604	38.27	-27.84	2.7557	1.3277	1.4281	0.0914	1.79	0.0447
H2	O8	65503	7.95	-5.18	2.7684	1.2005	1.5843	0.0279	0.39	0.4670
H4	O6	54503	9.70	-7.29	2.7387	1.2174	1.5328	0.0426	0.44	0.0226
O8	K1	55402	32.08	-22.59	2.8084	1.3503	1.4581	0.0770	1.53	0.0031
H10	O2	54501	70.16	-76.37	1.7520	0.5632	1.1888	0.2327	2.35	0.0060
N2	C9	54604	1.61	-0.91	4.0511	2.1250	2.0998	0.0065	0.08	1.0520
H1A	O7	65503	3.39	-2.25	3.3278	1.5918	1.7383	0.0174	0.17	1.2808
H1B	H4	55503	5.21	-3.32	2.5228	1.2079	1.3260	0.0205	0.26	1.1244
O9	K1	54501	39.58	-27.73	2.7246	1.2943	1.4305	0.0865	1.89	0.0041
C8	O3	55604	9.96	-7.21	3.4017	1.8345	1.5785	0.0404	0.47	1.1255
C8	O6	55502	6.63	-4.37	3.7811	2.0841	1.7149	0.0258	0.33	1.4057
H5	H1A	64503	5.04	-4.05	2.4024	1.2728	1.1722	0.0322	0.22	0.1443
H4	H1B	54503	5.21	-3.32	2.5228	1.3260	1.2079	0.0205	0.26	1.1244
C8	C6	44604	4.31	-3.12	3.6957	1.9960	1.7632	0.0245	0.20	0.8518
H8	H2	55502	8.55	-6.58	2.0333	1.0759	1.1435	0.0411	0.39	1.2895
H3	O2	45604	1.97	-1.19	3.6492	1.7597	1.9094	0.0096	0.10	0.2986
H1A	O4	55604	8.98	-6.09	2.6665	1.1425	1.5974	0.0330	0.44	0.5125
H1A	O4	55402	8.98	-6.09	2.6665	1.1426	1.5974	0.0330	0.44	0.5120
H4	O9	44604	2.48	-1.41	3.2831	1.5319	1.8119	0.0086	0.13	0.6513
O2	H10	44604	70.15	-76.37	1.7520	1.1888	0.5632	0.2327	2.35	0.0063
O7	K1	55402	34.42	-24.45	2.8087	1.3620	1.4470	0.0818	1.63	0.0054
O6	K1	45604	37.20	-26.70	2.7656	1.3324	1.4333	0.0875	1.75	0.0103
C8	O3	55402	9.96	-7.21	3.4017	1.8345	1.5785	0.0404	0.47	1.1255
O1	H9	55501	12.42	-7.79	2.4968	1.5517	1.0717	0.0329	0.63	2.3790
O5	H9	55501	41.65	-32.52	2.3200	1.3181	1.0301	0.1091	1.86	0.2710
C9	H3	55501	6.37	-4.59	2.9285	1.8541	1.2244	0.0306	0.30	0.0671

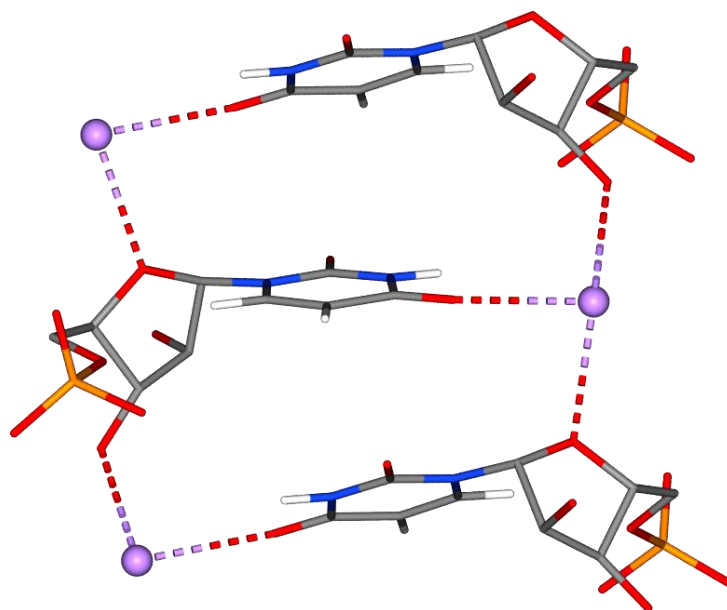


Figure 7S. Neighbourhood of uracil moiety in the direction perpendicular to the ring. Distance between the rings' centroids amounts to 4.156 Å.